Parthenogenetic chimaerism/mosaicism with a Silver-Russell syndrome-like phenotype

K Yamazawa,[1,2] K Nakabayashi,[3] M Kagami,[1] T Sato,[1] S Saitoh,[4] R Horikawa,[5] N Hizuka,[6] T Ogata[1]

► Additional figures, tables and an appendix are published online only. To view these files, please visit the journal online (http://jmg.bmj.com).

[1]Departments of Endocrinology and Metabolism, National Research Institute for Child Health and Development, Tokyo, Japan
[2]Department of Physiology, Development & Neuroscience, University of Cambridge, Cambridge, UK
[3]Maternal-Fetal Biology, National Research Institute for Child Health and Development, Tokyo, Japan
[4]Department of Pediatrics, Hokkaido University Graduate School of Medicine, Sapporo, Japan
[5]Division of Endocrinology and Metabolism, National Children's Hospital, Tokyo, Japan
[6]Department of Medicine, Institute of Clinical Endocrinology, Tokyo Women's Medical University, Tokyo, Japan

Correspondence to
Dr Tsutomu Ogata, Department of Endocrinology and Metabolism, National Research Institute for Child Health and Development, 2-10-1 Ohkura, Setagaya, Tokyo 157-8535, Japan; tomogata@nch.go.jp

Received 20 March 2010
Revised 6 May 2010
Accepted 8 May 2010
Published Online First 3 August 2010

ABSTRACT

Introduction We report a 34-year-old Japanese female with a Silver-Russell syndrome (SRS)-like phenotype and a mosaic Turner syndrome karyotype (45,X/46,XX).

Methods/Results Molecular studies including methylation analysis of 17 differentially methylated regions (DMRs) on the autosomes and the *XIST*-DMR on the X chromosome and genome-wide microsatellite analysis for 96 autosomal loci and 30 X chromosomal loci revealed that the 46,XX cell lineage was accompanied by maternal uniparental isodisomy for all chromosomes (upid(AC)mat), whereas the 45,X cell lineage was associated with biparentally derived autosomes and a maternally derived X chromosome. The frequency of the 46,XX upid(AC)mat cells was calculated as 84% in leukocytes, 56% in salivary cells, and 18% in buccal epithelial cells.

Discussion The results imply that a parthenogenetic activation took place around the time of fertilisation of a sperm missing a sex chromosome, resulting in the generation of the upid(AC)mat 46,XX cell lineage by endoreplication of one blastomere containing a female pronucleus and the 45,X cell lineage by union of male and female pronuclei. It is likely that the extent of overall (epi)genetic aberrations exceeded the threshold level for the development of SRS phenotype, but not for the occurrence of other imprinting disorders or recessive Mendelian disorders.

Although a mammal with maternal uniparental disomy for all chromosomes (upd(AC)mat) is incompatible with life because of genomic imprinting,[1] a mammal with a upd(AC)mat cell lineage could be viable in the presence of a co-existing normal cell lineage. In the human, Strain *et al*[2] have reported 46,XX peripheral blood cells with maternal uniparental isodisomy for all chromosomes (upid(AC)mat) in a 1.2-year-old phenotypically male patient with aggressive behaviour, hemifacial hypoplasia and normal birth weight. Because of the 46,XX disorders of sex development, detailed molecular studies were performed, revealing the presence of a normal 46,XY cell lineage in a vast majority of skin fibroblasts and a upid(AC)mat 46,XX cell lineage in nearly all blood cells. In addition, although the data are insufficient to draw a definitive conclusion, Horike *et al*[3] have also identified 46,XX peripheral blood cells with possible upd(AC)mat in a phenotypically male patient through methylation analyses for plural differentially methylated regions (DMRs) in 11 patients with Silver–Russell syndrome (SRS)-like phenotype. This patient was found to have a normal 46,XY cell lineage and a triploid 69,XXY cell lineage in skin fibroblasts.

However, such patients with a upd(AC)mat cell lineage remain extremely rare, and there is no report describing a human with such a cell lineage in the absence of a normal cell lineage. Here, we report a female patient with a upid(AC)mat 46,XX cell lineage and a non-upd 45,X cell lineage who was identified through genetic screenings of 103 patients with SRS-like phenotype.

MATERIALS AND METHODS

Case report

This Japanese female patient was conceived naturally and born at 40 weeks of gestation by a normal vaginal delivery. At birth, her length was 44.0 cm (−3.1 SD), her weight 2.1 kg (−2.9 SD) and her occipitofrontal head circumference (OFC) 30.5 cm (−2.3 SD). The parents and the younger brother were clinically normal (the father died from a traffic accident).

At 2 years of age, she was referred to us because of growth failure. Her height was 77.7 cm (−2.5 SD), her weight 8.45 kg (−2.6 SD) and her OFC 43.5 cm (−2.5 SD). Physical examination revealed several SRS-like somatic features such as triangular face, right hemihypoplasia and bilateral fifth finger clinodactyly. She also had developmental retardation, with a developmental quotient of 56. Endocrine studies for short stature were normal as were radiological studies. Cytogenetic analysis using lymphocytes indicated a low-grade mosaic Turner syndrome (TS) karyotype, 45,X[3]/46,XX[47]. Thus, a screening of TS phenotype[4] was performed, detecting horseshoe kidney but no body surface features or cardiovascular lesion. Chromosome analysis was repeated at 6 and 32 years of age using lymphocytes, revealing a 45,X[8]/46,XX[92] karyotype and a 45,X[12]/46,XX[88] karyotype, respectively. On the last examination at 34 years of age, her height was 125.0 cm (−6.2 SD), her weight 37.5 kg (−2.0 SD) and her OFC 51.2 cm (−2.8 SD). She was engaged in a simple work and was able to get on her daily life for herself.

Sample preparation

This study was approved by the Institutional Review Board Committees at National Center for Child health and Development. After obtaining written informed consent, genomic DNA was extracted from leukocytes of the patient, the mother and the brother and from salivary cells, which comprise ~40% of buccal epithelial cells and ~60% of leukocytes,[5] of the patient. Lymphocyte metaphase spreads and leukocyte RNA were also

obtained from the patient. Leukocytes of healthy adults and patients with imprinting disorders were utilised for controls.

Primers and probes

The primers utilised in this study are summarised in supplementary methods and supplementary tables 1–3.

DMR analyses

We first performed bio-combined bisulfite restriction analysis (COBRA)[6] and bisulfite sequencing of the *H19*-DMR (A) on chromosome 11p15.5 by the previously described methods[7] and methylation-sensitive PCR analysis of the *MEST*-DMR (A) on chromosome 7q32.2 by the previously described methods[8] with minor modifications (the methylated and unmethylated allele-specific primers were designed to yield PCR products of different sizes, and the PCR products were visualised on the 2100 Bioanalyzer (Agilent, Santa Clara, California, USA)). This was because hypomethylation (epimutation) of the normally methylated *H19*-DMR of paternal origin and maternal uniparental disomy 7 are known to account for 35–65% and 5–10% of SRS patients, respectively.[9 10] In addition, fluorescence in situ hybridisation (FISH) analysis was performed with a ~84-kb RP5-998N23 probe containing the *H19*-DMR (BACPAC Resources Center, Oakland, California, USA). We also examined multiple other DMRs by bio-COBRA. The ratio of methylated clones (the methylation index) was calculated using peak heights of digested and undigested fragments on the 2100 Bioanalyzer using 2100 expert software.

Genome-wide microsatellite analysis

Microsatellite analysis was performed for 96 autosomal loci and 30 X chromosomal loci. The segment encompassing each locus was PCR-amplified, and the PCR product size was determined on the ABI PRISM 310 autosequencer using GeneScan software (Applied Biosystems, Foster City, California, USA).

PCR analysis for Y chromosomal loci

Standard PCR was performed for six Y chromosomal loci. The PCR products were electrophoresed using the 2100 Bioanalyzer.

Expression analysis

Quantitative real-time reverse transcriptase PCR analysis was performed for three paternally expressed genes (*IGF2*, *SNRPN* and *ZAC1*) and four maternally expressed genes (*H19*, *MEG3*, *PHLDA2* and *CDKN1C*) that are known to be variably (usually weakly) expressed in leukocytes (UniGene, http://www.ncbi.nlm.nih.gov/sites/entrez?db=unigene), using an ABI Prism 7000 Sequence Detection System (Applied Biosystems). *TBP* and *GAPDH* were utilised as internal controls.

RESULTS

DMR analyses

In leukocytes, the bio-COBRA indicated severely hypomethylated *H19*-DMR, and bisulfite sequencing combined with *rs2251375* SNP typing for 30 clones revealed maternal origin of 29 hypomethylated clones and non-maternal (paternal) origin of a single methylated clone in this patient (figure 1A). Thus, the marked hypomethylation of the *H19*-DMR was caused by predominance of maternally derived clones rather than hypomethylation of the *H19*-DMR of paternal origin. FISH analysis for 100 lymphocyte metaphase spreads excluded an apparent deletion of the paternally derived *H19*-DMR or duplication of the maternally derived *H19*-DMR (Supplementary figure 1). Methylation-sensitive PCR amplification for the *MEST*-DMR delineated a major peak for the methylated allele and a minor peak for the unmethylated allele (figure 1B). This also indicated the predominance of maternally derived clones and the co-existence of a minor portion of paternally derived clones. Furthermore, autosomal DMRs invariably exhibited markedly abnormal methylation patterns consistent with predominance of maternally inherited DMRs, whereas the methylation index of the *XIST*-DMR on the X chromosome remained within the female reference range (figure 1C). The abnormal methylation patterns were less obvious in salivary cells (thus, in buccal epithelial cells) than in leukocytes, except for the methylation index for the *XIST*-DMR that mildly exceeded the female reference range (figure 1A–C).

Microsatellite analysis

Major peaks consistent with maternal uniparental isodisomy and minor peaks of non-maternal (paternal) origin were identified for at least one locus on each autosome, with the minor peaks of non-maternal origin being more obvious in salivary cells than in leukocytes (figure 1D and supplementary table 4). Furthermore, the frequency of the upid(AC)mat cells was calculated as 84% in leukocytes, 56% in salivary cells and 18% in epithelial buccal cells, using the area under curves for the maternally and the non-maternally inherited peaks (supplementary note). Such minor peaks of non-maternal origin were not detected for all the 30 X chromosomal loci examined.

PCR analysis for Y chromosomal loci

PCR amplification failed to detect any trace of Y chromosome-specific bands in leukocytes and salivary cells (Supplementary figure 2).

Expression analysis

Expression analysis using control leukocytes indicated that, of the seven examined genes, *SNRPN* expression alone was strong enough to allow for a precise assessment (Supplementary figure 3). *SNRPN* expression was extremely low in this patient (figure 1E).

DISCUSSION

These results imply that this patient had a upid(AC)mat 46,XX cell lineage and a non-upd 45,X cell lineage. Indeed, methylation patterns of the *XIST*-DMR is explained by assuming that the two X chromosomes in the upid(AC)mat cells undergo random X-inactivation and that 45,X cells with the methylated *XIST*-DMR on a single active X chromosome[11] are relatively prevalent in buccal epithelial cells. Furthermore, lack of non-maternally derived minor peaks for microsatellite loci on the X chromosome is explained by assuming that the two X chromosomes in the upid(AC)mat cells and the single X chromosome in the 45,X cells are derived from a common X chromosome of maternal origin, with no paternally derived sex chromosome. It is likely, therefore, that a parthenogenetic activation took place around the time of fertilisation of a sperm missing a sex chromosome, resulting in the generation of the 46,XX cell lineage with upid (AC)mat by endoreplication (the replication of DNA without the subsequent completion of mitosis) of one blastomere containing a female pronucleus and the 45,X cell lineage with biparentally derived autosomes and a maternally derived X chromosome by union of male and female pronuclei (figure 2), although it is also possible that a paternally derived sex chromosome was present in the sperm but was lost from the normal

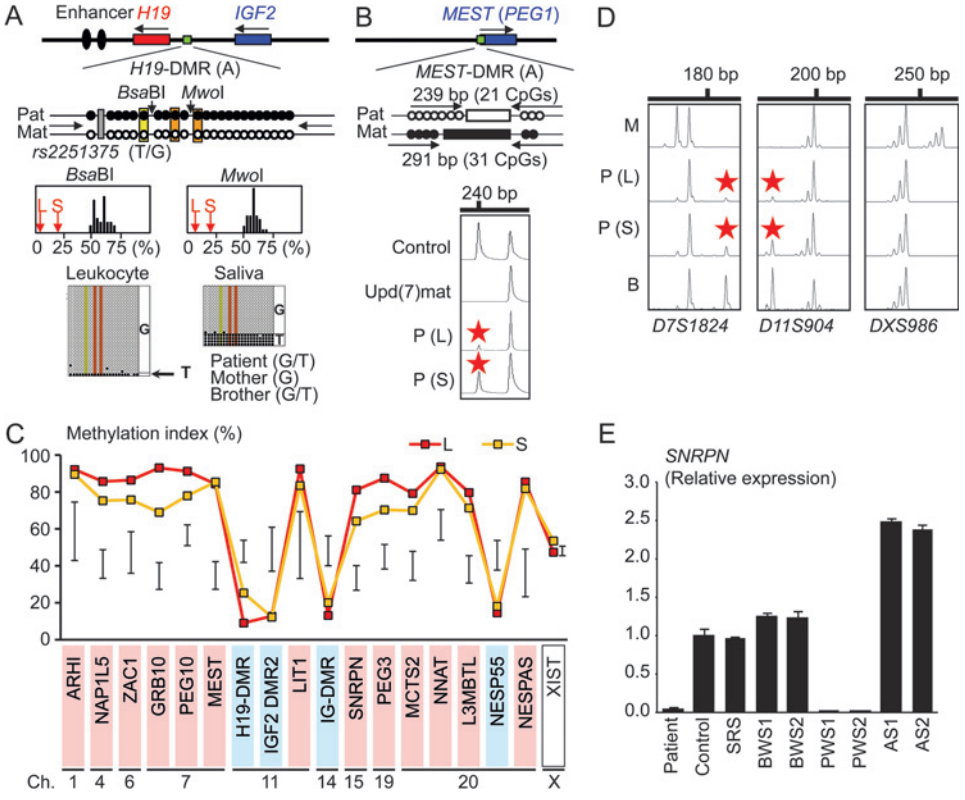

Figure 1 Representative molecular results. Pat, paternally derived allele; Mat, maternally derived allele; P, patient; M, mother; B, brother; L, leukocytes; and S, salivary cells. Filled and open circles in A and B represent methylated and unmethylated cytosine residues at the CpG dinucleotides, respectively. A. Methylation patterns of the *H19*-DMR (A) harbouring 23 CpG dinucleotides and the T/G SNP (*rs2251375*) (a grey box). The PCR products are digested with *Bsa*BI when the cytosine at the sixth CpG dinucleotide (highlighted in yellow) is methylated and with *Mwo*I when the two cytosines at the ninth and the 11th CpG dinucleotides (highlighted in orange) are methylated. For the bio-COBRA data, the black histograms represent the distribution of methylation indices (%) in 50 control participants, and L and S denote the methylation indices for leukocytes and salivary cells of this patient, respectively. For the bisulfite sequencing data, each line indicates a single clone. B. Methylated and unmethylated allele-specific PCR analysis for the *MEST*-DMR (A). In a control participant, the PCR products for methylated and unmethylated alleles are delineated, and the unequal amplification is consistent with a short product being more easily amplified than a long product. In a previously reported patient with upd(7)mat,[8] the methylated allele only is amplified. In this patient, major peaks for the methylated allele and minor peaks for the unmethylated allele (red asterisks) are detected. C. Methylation patterns for the 18 DMRs examined. The DMRs highlighted in blue and pink are methylated after paternal and maternal transmissions, respectively. The black vertical bars indicate the reference data (maximum—minimum) in 20 normal control participants, using leukocyte genomic DNA (for the *XIST*-DMR, 16 female data are shown). D. Representative microsatellite analysis. Minor peaks (red asterisks) have been identified for *D7S1824* and *D11S904* but not for *DXS986* of the patient. Since the peaks for *D7S1824* and *D11S904* are absent in the mother and clearly present in the brother, they are assessed to be of paternal origin. E. Relative expression level (mean ± SD) of *SNRPN* on chromosome 15. The data have been normalised against *TBP*. SRS, an SRS patient with an epimutation (hypomethylation) of the *H19*-DMR; BWS1, a BWS patient with an epimutation (hypermethylation) of the *H19*-DMR; BWS2, a BWS patient with upd(11)pat; PWS1, a PWS patient with upd(15)mat; PWS2, a PWS patient with an epimutation (hypermethylation) of the *SNRPN*-DMR; AS1, an Angelman syndrome (AS) patient with upd(15)pat; and AS2, an AS patient with an epimutation (hypomethylation) of the *SNRPN*-DMR.

cell lineage at the very early developmental stage. Hence, in a strict sense, this patient is neither a chimera resulting from the fusion of two different zygotes nor a mosaic caused by a mitotic error of a single zygote. In this regard, a triploid cell stage is assumed in the generation of a upid(AC)mat cell lineage, and such triploid cells may have been detected in skin fibroblasts of the patient reported by Horike *et al*.[3]

The upid(AC)mat cells accounted for the majority of leukocytes even in adulthood of this patient, despite global negative selective pressure.[12 13] This phenomenon, though intriguing, would not be unexpected in human studies because leukocytes are usually utilised for genetic analyses. Rather, if the upid(AC)mat cells were barely present in leukocytes, they would not have been detected. It is likely, therefore, that upid(AC)mat cells have occupied a relatively large portion of the definitive haematopoietic tissues primarily as a stochastic event. Furthermore, parthenogenetic chimera mouse studies have revealed that parthenogenetic cells are found at a relatively high frequency in some tissues/organs including blood and are barely identified in other tissues/organs such as skeletal muscle and liver.[13] Such a possible tissue-specific selection in favour of the preservation of parthenogenetic cells in the definitive haematopoietic tissues may also be relevant to the predominance of the upid(AC)mat cells in leukocytes. In addition, a reduced growth potential of 45,X cells[14] may also have contributed to the skewed ratio of the two cell lineages.

Clinical features of this patient would be determined by several factors. They include: (1) the ratio of two cell lineages in various tissues/organs, (2) the number of imprinted regions or DMRs relevant to the development of specific imprinting disorders (eg, plural regions/DMRs on chromosomes 7 and 11 for SRS[9 10] and a single region/DMR on chromosome 15 for Prader—Willi syndrome (PWS)),[15] (3) the degree of clinical effects of dysregulated imprinted regions/DMRs (an (epi)dominant effect has been

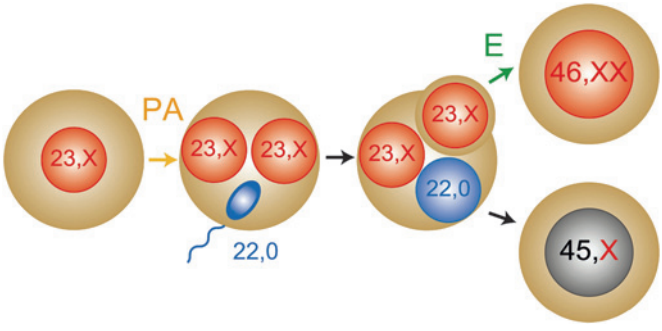

Figure 2 Schematic representation of the generation of the upid(AC)mat 46,XX cell lineage and the non-upd 45,X cell lineage. Polar bodies are not shown. PA, parthenogenetic activation; and E, endoreplication of one blastomere containing a female pronucleus.

assumed for the 11p15.5 imprinted regions including the *IGF2–H19* domain on the basis of SRS or Beckwith–Wiedemann syndrome (BWS) phenotype in patients with multilocus hypomethylation[16] and BWS-like phenotype in patients with a upid (AC)pat cell lineage,[17] a mirror image of a upid(AC)mat cell lineage), (4) expression levels of imprinted genes in upid(AC)mat cells (although *SNRPN* expression of this patient was consistent with upid(AC)mat cells being predominant in leukocytes, complicated expression patterns have been identified for several imprinted genes in androgenetic and parthenogenetic fetal mice, probably because of perturbed *cis*- and *trans*-acting regulatory mechanisms)[18] and (5) unmasking of possible maternally inherited recessive mutation(s) in upid(AC)mat cells.[19] Collectively, it appears that the extent of overall (epi)genetic aberrations exceeded the threshold level for the development of SRS phenotype and horseshoe kidney characteristic of TS[4] but remained below the threshold level for the occurrence of other imprinting disorders or recessive Mendelian disorders.

In summary, we identified a upid(AC)mat 46,XX cell lineage in a woman with an SRS-like phenotype and a 45,X cell lineage accompanied by autosomal haploid sets of biparental origin. This report will facilitate further identification of patients with a upid(AC)mat cell lineage and better clarification of the clinical phenotypes in such patients.

Acknowledgements We thank the patient and her family members for their participation in this study. We also thank Dr. Toshiro Nagai for providing us with blood samples of patients with Prader–Willi syndrome.

Funding This work was supported by grants from the Ministry of Health, Labor, and Welfare and from the Ministry of Education, Science, Sports and Culture.

Competing interests None.

Patient consent Obtained.

Ethics approval This study was conducted with the approval of the Institutional Review Board Committees at National Center for Child health and Development.

Contributors Drs Kazuki Yamazawa (first author) and Kazuhiko Nakabayashi (second author) contributed equally to this work.

Provenance and peer review Not commissioned; externally peer reviewed.

REFERENCES

1. **McGrath J,** Solter D. Completion of mouse embryogenesis requires both the maternal and paternal genomes. *Cell* 1984;**37**:179–83.
2. **Strain L,** Warner JP, Johnston T, Bonthron DT. A human parthenogenetic chimaera. *Nat Genet* 1995;**11**:164–9.
3. **Horike S,** Ferreira JC, Meguro-Horike M, Choufani S, Smith AC, Shuman C, Meschino W, Chitayat D, Zackai E, Scherer SW, Weksberg R. Screening of DNA methylation at the H19 promoter or the distal region of its ICR1 ensures efficient detection of chromosome 11p15 epimutations in Russell–Silver syndrome. *Am J Med Genet Part A* 2009;**149A**:2415–23.
4. **Styne D,** Grumbach M. Puberty: ontogeny, neuroendocrinology, physiology, and disorders. In: Kronenberg H, Melmed M, Polonsky K, Larsen P, eds. *Williams textbook of endocrinology*, 11th edn. Philadelphia: Saunders 2008:969–1166.
5. **Thiede C,** Prange-Krex G, Freiberg-Richter J, Bornhauser M, Ehninger G. Buccal swabs but not mouthwash samples can be used to obtain pretransplant DNA fingerprints from recipients of allogeneic bone marrow transplants. *Bone Marrow Transplant* 2000;**25**:575–7.
6. **Brena RM,** Auer H, Kornacker K, Hackanson B, Raval A, Byrd JC, Plass C. Accurate quantification of DNA methylation using combined bisulfite restriction analysis coupled with the Agilent 2100 Bioanalyzer platform. *Nucleic Acids Res* 2006;**34**:e17.
7. **Yamazawa K,** Kagami M, Nagai T, Kondoh T, Onigata K, Maeyama K, Hasegawa T, Hasegawa Y, Yamazaki T, Mizuno S, Miyoshi Y, Miyagawa S, Horikawa R, Matsuoka K, Ogata T. Molecular and clinical findings and their correlations in Silver–Russell syndrome: implications for a positive role of IGF2 in growth determination and differential imprinting regulation of the IGF2-H19 domain in bodies and placentas. *J Mol Med* 2008;**86**:1171–81.
8. **Yamazawa K,** Kagami M, Ogawa M, Horikawa R, Ogata T. Placental hypoplasia in maternal uniparental disomy for chromosome 7. *Am J Med Genet Part A* 2008;**146A**:514–16.
9. **Abu-Amero S,** Monk D, Frost J, Preece M, Stanier P, Moore GE. The genetic aetiology of Silver–Russell syndrome. *J Med Genet* 2008;**45**:193–9.
10. **Eggermann T,** Eggermann K, Schonherr N. Growth retardation versus overgrowth: Silver–Russell syndrome is genetically opposite to Beckwith–Wiedemann syndrome. *Trends Genet* 2008;**24**:195–204.
11. **Goto T,** Monk M. Regulation of X-chromosome inactivation in development in mice and humans. *Microbiol Mol Biol Rev* 1998;**62**:362–78.
12. **Nagy A,** Sass M, Markkula M. Systematic non-uniform distribution of parthenogenetic cells in adult mouse chimaeras. *Development* 1989;**106**:321–4.
13. **Fundele R,** Norris ML, Barton SC, Reik W, Surani MA. Systematic elimination of parthenogenetic cells in mouse chimeras. *Development* 1989;**106**:29–35.
14. **Verp MS,** Rosinsky B, Le Beau MM, Martin AO, Kaplan R, Wallemark CB, Otano L, Simpson JL. Growth disadvantage of 45, X and 46, X, del(X)(p11) fibroblasts. *Clin Genet* 1988;**33**:277–85.
15. **Horsthemke B,** Wagstaff J. Mechanisms of imprinting of the Prader–Willi/Angelman region. *Am J Med Genet A* 2008;**146A**:2041–52.
16. **Azzi S,** Rossignol S, Steunou V, Sas T, Thibaud N, Danton F, Le Jule M, Heinrichs C, Cabrol S, Gicquel C, Le Bouc Y, Netchine I. Multilocus methylation analysis in a large cohort of 11p15-related foetal growth disorders (Russell Silver and Beckwith Wiedemann syndromes) reveals simultaneous loss of methylation at paternal and maternal imprinted loci. *Hum Mol Genet* 2009;**18**:4724–33.
17. **Wilson M,** Peters G, Bennetts B, McGillivray G, Wu ZH, Poon C, Algar E. The clinical phenotype of mosaicism for genome-wide paternal uniparental disomy: two new reports. *Am J Med Genet Part A* 2008;**146A**:137–48.
18. **Ogawa H,** Wu Q, Komiyama J, Obata Y, Kono T. Disruption of parental-specific expression of imprinted genes in uniparental fetuses. *FEBS Lett* 2006;**580**:5377–84.
19. **Engel E.** A fascination with chromosome rescue in uniparental disomy: Mendelian recessive outlaws and imprinting copyrights infringements. *Eur J Hum Genet* 2006;**14**:1158–69.

SUPPLEMENTARY MATERIALS

A 46,XX Cell Lineage with Maternal Uniparental Isodisomy for All Chromosomes in a Female with a Silver-Russell Syndrome-like Phenotype and a 45,X Turner Cell Lineage Accompanied by Biparentally Derived Autosomes

Kazuki Yamazawa,[1,*,†] Kazuhiko Nakabayashi,[2,*] Masayo Kagami,[1] Tomoko Sato,[1] Shinji Saitoh,[3] Reiko Horikawa,[4] Naomi Hizuka,[5] Tsutomu Ogata[1]

Departments of [1]Endocrinology and Metabolism, and [2]Maternal-Fetal Biology, National Research Institute for Child Health and Development, Tokyo, Japan; [3]Department of Pediatrics, Hokkaido University Graduate School of Medicine, Sapporo, Japan; [4]Division of Endocrinology and Metabolism, National Children's Hospital, Tokyo, Japan; [5]Department of Medicine, Institute of Clinical Endocrinology, Tokyo Women's Medical University, Tokyo, Japan

Correspondence to: Dr T Ogata, Department of Endocrinology and Metabolism, National Research Institute for Child Health and Development, 2-10-1 Ohkura, Setagaya, Tokyo 157-8535, Japan. Tel: +81-3-5494-7025; Fax: +81-3-5494-7026; E-mail: tomogata@nch.go.jp

*These authors contributed equally to this work.

[†]Present address: Department of Physiology, Development & Neuroscience, University of Cambridge, Cambridge, UK

SUPPLEMENTARY METHODS

Primers

The primers for bisulfite-PCR assays utilized for genetic screenings for Silver-Russell syndrome are shown in supplementary table 1, those for bio-COBRA (combined bisulfite restriction analysis) assays for multiple DMRs (differentially methylated regions) are shown in supplementary table 2, and those for Y chromosome analysis are shown in supplementary table 3. The primers for genomewide microsatellite analysis were based on ABI PRISM Linkage Mapping Set v2.5-MD10 (Applied Biosystems, Foster City, California, USA), and loci with high heterozygosities in the Japanese population were examined.[1] The probe-primer mixtures for quantitative real-time reverse transcriptase PCR analysis were as follows (assay IDs): Hs01005963_m1 for *IGF2*, Hs00256090_m1 for *SNRPN*, Hs00414677_m1 for *ZAC1*, Hs00399294_g1 for *H19*, Hs00292028_m1 for *MEG3*, Hs00169368_m1 for *PHLDA2*, and Hs00175938_m1 for *CDKN1C* (Applied Biosystems); the TATA box binding protein (*TBP*) and glyceraldehyde-3-phosphate dehydrogenase (*GAPDH*) were used as internal controls, using the Human TBP Endogenous Control and Human GAPDH Endogenous Control, respectively (Applied Biosystems).

Supplementary Table 1. Bisulfite-PCR primers utilized for genetic screenings for Silver-Russell syndrome

DMR	Nucleotide positions*	Forward primer sequence (5' → 3') / Reverse primer sequence (5' → 3')	AT / PS
H19-DMR (A)	1976042–1976360 (–)	AACCCCTTCCTACCACCATC	60
		GGGTTTGGGAGAGTTTGTGA	317
MEST-DMR (A) (methylated allele)	129919201–129919491 (+)	TAGTTGCGTTTCGTAAGGTAGTGTC	58
		ACACAATCCTCCGCTCGCCTA	291
MEST-DMR (A) (unmethylated allele)	129919254–129919492 (+)	GTTTGGTGTGGTGTTGTTTTGTGTGGG	60
		CACACAATCCTCCACTCACCTACA	239

*Nucleotide positions are based on the human reference sequence assembly (NCBI Build 36.1); The (+) and the (–) symbols after nucleotide positions indicate the DNA strand utilized to design PCR primers.

AT: Annealing temperature (°C), PS: product size (bp).

The primer sequences and PCR conditions for *H19*-DMR (A) and the *MEST*-DMR (A) (methylated allele) have been reported previously[2, 3], whereas those for the *MEST*-DMR (A) (unmethylated allele) are designed in this study.

Supplementary Table 2. Bisulfite-PCR primers and restriction enzymes utilized for bio-COBRA assays

DMR	Chromosome number Nucleotide positions*	Forward primer sequence (5' → 3') Reverse primer sequence (5' → 3')	AT PS	Enzyme† Frag. size
ARHI-DMR	Chromosome 1	GGTTTTAAGGAATAGAAGTTGTTGA	55	*Bst*UI
	68285331–68285550 (–)	AACCCAACAACTAACAATAAATATTTT	220	122/62/36
NAP1L5-DMR	Chromosome 4	GGGGTTTTTTAGTTATTTGATTAGT	55	*Taq*I
	89837763–89838003 (+)	AAAATCTCTCTAAACCAACTC	241	154/65/22
ZAC1-DMR	Chromosome 6	GGGGTAGTYGTGTTTATAGTTTAGTA	62	*Taq*I
	144370901–144371052 (–)	CRAACACCCAAACACCTACCCT	152	91/61
GRB10-DMR	Chromosome 7	GTTATATAATATTGTTTTATGGTTGG	57	*Taq*I
	50817378–50817623 (+)	GCTCTCCAAATACTCAAATAAACTCC	246	158/88
PEG10-DMR	Chromosome 7	GGTTTTTTTATTTGTTTTGGGGTATA	57	*Taq*I
	94123783–94123981 (–)	ATATAAAACCCCATCCTTCCTATCTT	199	106/93
MEST-DMR‡	Chromosome 7	TYGTTGTTGGTTAGTTTTGTAYGGTT	57	*Taq*I
	129919303–129919521 (+)	CCCAAAAACAACCCCAACTC	219	101/97/21
H19-DMR‡	Chromosome 11	GAGTTYGGGGGTTTTTGTATAGT	60	*Taq*I
	1977615–1977893 (–)	TAAATAATACCCRACCTAAAAATCTAA	279	142/137
IGF2-DMR2	Chromosome 11	ATTGTTGGTTATTTTTGGGGG	57	*Taq*I
	2,110,802–2,111,138 (+)	AACTCAAATCACTAATCAATCACAAAA	337	242/95
LIT1-DMR	Chromosome 11	TTTTGGTAGGATTTTGTTGAGGAGT	57	*Bst*UI
	2677736–2678042 (+)	CCTCACACCCAACCAATACCTC	307	255/52
IG-DMR-CG4	Chromosome 14	AATTATTTTTTGGATAAGAGAGTATA	57	*Bst*UI
	100345398–100345600 (+)	ATTACAAACCAAAATAAAATATAATAAATC	203	123/62/18
SNRPN-DMR	Chromosome 15	AGGGAGTTGGGATTTTTGTATTG	57	*Rsa*I
	22751048–22751345 (+)	CTCCCCAAACTATCTCTTAAAAAAAACC	240	205/35
PEG3-DMR	Chromosome 19	AAAAGGTATTAATTATTTATAGTTTGGT	57	*Taq*I
	62043541–62043862 (+)	AAAAATATCCACCCTAAACTAATAA	322	206/116
MCTS2-DMR	Chromosome 20	GTTAGAATTAATTTATTAGGGTG	57	*Taq*I
	29598611–29598909 (+)	AAATCCCCTACAAAAAAACC	299	172/127
NNAT-DMR	Chromosome 20	ATTTTTTTTGTATTTTTTTTATAGATAT	55	*Mlu*I
	35582379–35582576	ATTTTAAACCCAAATCCTCTACTTC	197	153/44
L3MBTL-DMR	Chromosome 20	GGTTTAGTTAATTTTTATAGATATTGATT	57	*Bst*UI
	41575924–41576143 (–)	ACCCTAAATATATCTTACTTTCCCC	220	163/57
NESP55-DMR	Chromosome 20	GTTTTTTTGGTTTTTTTGTTTTAT	57	*Taq*I
	56848649–56848844 (+)	AAACAACTCAAAATCTACCTCCTC	196	147/49
NESPAS-DMR	Chromosome 20	AATTTGTGGTATGAGGAAGAGTGAT	57	*Bst*UI
	56859212–56859446 (+)	TCAACCATTAAACAAAAATCATACC	235	130/105
XIST-DMR	Chromosome X	AAAATGTTTTAGAAAGAATTTTAAGTGTAG	57	*Taq*I
	72989197–72989403 (+)	AAATAAATTTTAAACCAACCAAATCAC	207	147/60

*Nucleotide positions are based on the human reference sequence assembly (NCBI Build 36.1); The (+) and the (–) symbols after nucleotide positions indicate the DNA strand utilized to design PCR primers.

†These enzymes digest methylated clones.

‡Note that the *MEST*-DMR examined with these primers is different from the *MEST*-DMR (A) examined with the primers shown in supplementary table 1; similarly, the *H19*-DMR examined with these primers contains the CTCF binding site 6 and is different from the *H19*-DMR (A) examined with the primers shown in supplementary table 1 that resides outside the CTCF binding sites.

AT: Annealing temperature (°C), PS: product size (bp); Y: C or T (pyrimidine) ; and R: A or G (purine).

The primer sequences have been designed by us, except for those for the following DMRs reported in the literature: the *ZAC1*-DMR,[4] the *MEST*-DMR, the *H19*-DMR,[5] the *LIT1*-DMR, the *SNRPN*-DMR,[6] and the *PEG3*-DMR.[7]

Supplementary Table 3. PCR primers and conditions utilized for sex chromosome analyses

Locus	Primer sequence (5' → 3')	AT	PS
PABY/*PABX*	GTACTACCTTTAGAAAACTAGTATTTTCCC (Y-specific)	54	950 (*PABY*)
	CTGCAGAAACAAGCTCATCAGCGTGACTAT (X-specific)		771 (*PABX*)
	GAATTCTTAACAGGACCCATTTAGGATTAA (common)		
SRY	GAATATTCCCGCTCTCCGGA	58	470
	GCTGGTGCTCCATTCTTGAGT		
ZFY/*ZFX*	CATCTTTACAAGCTTGTAGACACACT (Y-specific)	62	340 *(ZFY*)
	GAACACACTACTGAGCAAAATGTATA (X-specific)		488 (*ZFX*)
	ATTTGTTCTAAGTCGCCATATTCTCT (common)		
AMELY/*AMELX*	CTCTGATGGTTGGCCTCAAGCCTGT	62	618 (*AMELY*)
	CACTGTCCCTCATCCTAGAAACACA		804 (*AMELX*)
DYS14	GGGCCAATGTTGTATCCTTCTC	52	84
	GCCCATCGGTCACTTACACTTC		
DYZ3	TCCTTTTCCACAATAGACGTCA	58	174
	GGAAGTATCTTCCCTTAAAAGCTATG		

AT: annealing temperature (°C); and PS: product size (bp).

Supplementary Table 4. The results of microsatellite analysis

Locus	Mother	Patient	Brother	Locus	Mother	Patient	Brother
D1S238	295/309	309	295/305	*D13S170*	147/153	153/(163)	143/147
D1S207	148/166	166	164/166	*D13S153*	93/107	93/(97)	97/107
D1S218	275/277	(269)/275	269/275	*D14S72*	194/198	194/(198)	198/200
D1S2841	238/248	238/(248)	238/248	*D14S80*	98	98/(105)	98/103
D2S117	196/208	208/(210)	196/206	*D14S608*	204/214	204/(218)	214/218
D2S2330	170/172	170/(172)	172	*D14S588*	118/126	(114)/126	114/126
D2S2333	95/99	99/(103)	95/101	*D14S250*	161	161/(175)	161/175
D2S367	320/328	320/(328)	328	*D14S1010*	142/150	(148)/150	142/148
D3S1580	235	235	235/237	*D14S1007*	111	111/(119)	111/119
D3S1292	120/124	120/(128)	120/132	*D15S205*	161/163	163/(165)	157/163
D3S1566	165/167	167	167/175	*D15S1007*	88/90	88/(92)	90/92
D3S1263	195/201	195/(205)	201/215	*D15S128*	205/211	205	205/211
D4S1535	261	261	261/263	*D16S515*	336/338	(332)/338	332/336
D4S402	113/137	113/(131)	107/113	*D16S3091*	175/181	181/(185)	175/185
D4S1572	206/210	206	206	*D16S423*	136	136/(150)	136/150
D4S392	95/99	95/(101)	93/99	*D17S928*	82/86	86/(88)	86/88
D5S400	198/234	198/(234)	228/234	*D17S787*	145/155	155/(171)	145/163
D5S644	97/99	(95)/99	95/99	*D17S831*	116/118	(112)/118	112/118
D5S407	87/97	(83)/97	83/87	*D18S452*	125/129	125/(133)	125/131
D6S281	144/152	144/(152)	144/152	*D18S53*	170/172	170/(172)	170/172
D6S289	161	161	161	*D18S61*	229	(225)/229	225/229
D6S257	177	(175)/177	175/177	*D19S220*	279	(275)/279	275/279
D6S292	150/158	158/(168)	158/168	*D19S209*	244/252	(242)/244	242/244
D7S531	249	249/(251)	249/251	*D19S226*	252/254	(246)/254	246/254
D7S484	100/102	(98)/100	98/100	*D20S196*	263/288	263/(285)	263/285
D7S2846	176	176	176	*D20S117*	178/180	178/(180)	180
D7S519	264/266	(262)/264	262/264	*D20S186*	128/138	(116)/128	116/138
D7S672	132/148	(136)/148	132/136	*D21S266*	156/160	(156)/160	156/160
D7S669	124/130	124	124/130	*D21S1256*	102/110	(102)/110	102
D7S684	179	(167)/179	167/179	*D21S1252*	162	162/(168)	162/168
D7S1824	169/173	173/(185)	173/185	*D22S274*	284/292	292	292
D7S550	188	(186)/188	186/188	*D22S423*	298/308	298/(306)	298/306
D8S284	286/300	286	300/302	*D22S315*	195/197	(195)/197	195/197
D8S272	239	239	239/247	*SHOX**	153	153	151/153
D8S277	171/177	(167)/177	167/171	*DXYS85**	76	76	76
D8S264	143/145	145	143/145	*DXYS228**	199	199	199
D9S1677	240/242	242/(254)	242/254	*DXYS232**	170	170	170
D9S167	317/319	319	317/319	*DXYS10091**	214	214	214
D9S1817	288/296	296/(306)	288/306	*DXYS10083**	166/168	168	162/168
D9S157	227/239	227/(239)	239	*DXYS10086**	170/184	170	170/172
D10S537	155/157	(155)/157	155	*DXYS10096**	255/259	255	255
D10S249	131/133	(127)/131	127/133	*DXYS233**	164/168	168	168/170
D10S192	251/257	(253)/257	251/257	*DXS1047*	161	161	161
D11S2071	188	188	184/188	*DXS986*	246/258	246	246
D11S922	116/120	(90)/116	90/116	*DXS1060*	169/175	169	175
D11S1318	140	140	140	*DXS1226*	293/295	293	293
D11S4088	212/214	214	208/214	*DXS8051*	113	113	113
D11S988	117/125	(115)/117	117/127	*DXS1001*	200/204	204	200
D11S902	145/147	145	145	*DXS8055*	312/316	316	312
D11S904	198	(184)/198	184/198	*DXS1073*	308	308	308
D11S1918	186/194	(182)/186	182/194	*DXS8091*	86	86	86
D11S4083	179/193	193	179/191	*DXS990*	125/129	129	125
D11S4109	153/171	171	153/167	*DXS987*	214/222	222	222
D11S901	168	(166)/168	166/168	*DXS993*	270	270	270
D11S1356	191/217	(205)/217	191/205	*DXS1227*	81/83	83	83
D11S934	177/181	181	181	*DXS1068*	254/262	262	254
D11S912	96/100	100	100	*DXS1106*	130/132	130	132
D11S1304	175	175	175	*DXS8043*	149/155	155	155
D11S968	143	143	143	*DXS991*	328/332	332	328
D12S345	219/235	235	219/231	*DXS1214*	287/293	287	287
D12S1617	252/254	254/(262)	254/258	*DXYS227*†	124	124	124
D12S99	272	272/(274)	272/286	*DXYS154*†	244/248	244	244/246
D13S285	93/103	(95)/103	95/103	*DXYS225*†	210/214	214	214

The Arabic numbers represent the sizes of the PCR products in bp.
The numbers in parentheses of the patient are minor peaks of non-maternal (paternal) origin.
*Loci on the short arm pseudoautosomal region, and †those on the long arm pseudoautosomal region.

Supplementary Figure 1. FISH analysis of the *H19*-DMR

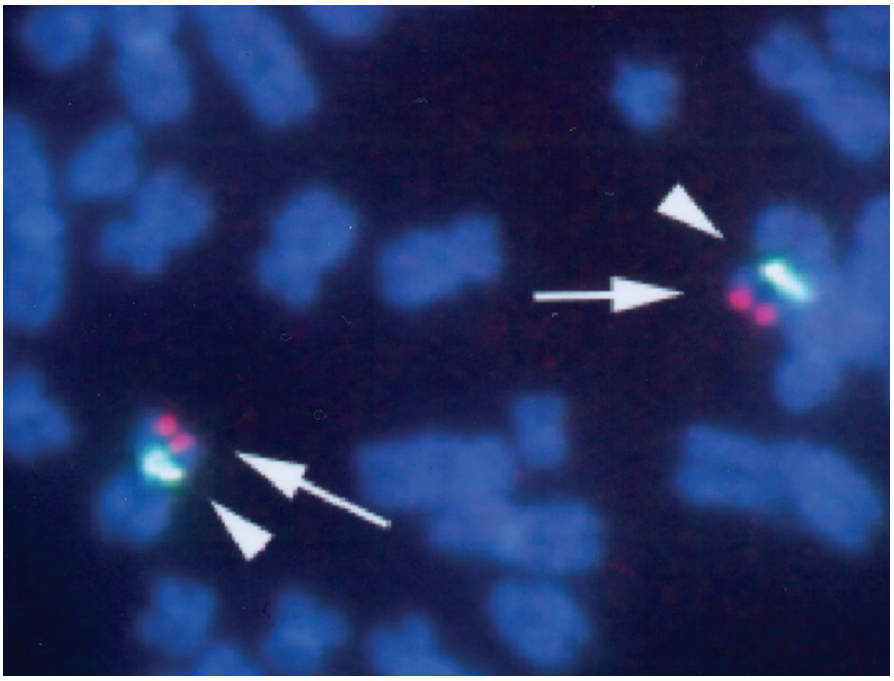

The RP5-998N23 has labeled with digoxigenin and detected by rhodamine anti-digoxigenin (red signals), and the control CEP 11 probe has been identified according to the manufacture's protocol (green signals).

Supplementary Figure 2. PCR analysis of Y-chromosomal loci

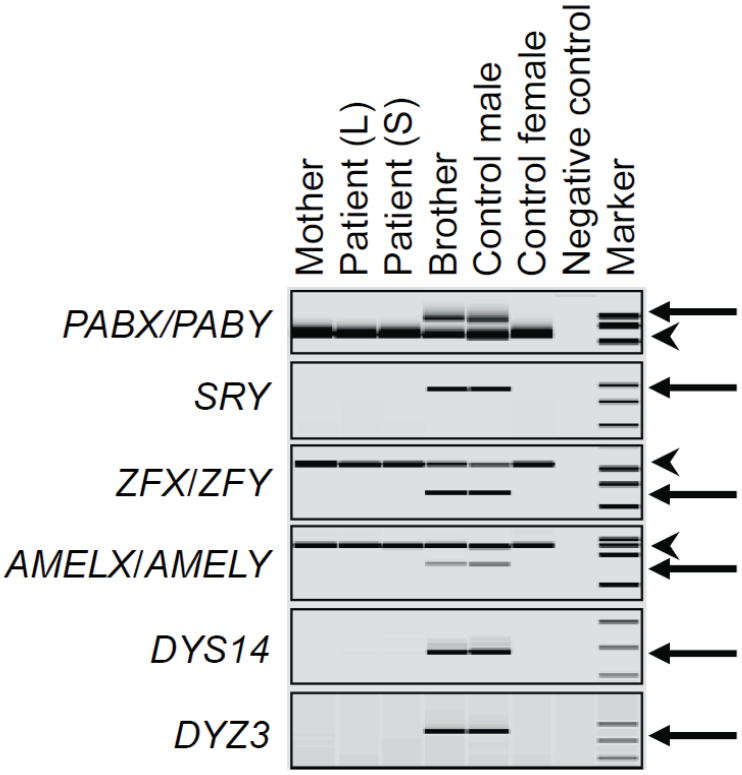

L: leukocytes; and S: salivary cells. No Y-specific bands (arrows) are identified whereas X-specific bands (arrowheads) are detected in both leukocytes and salivary cells of the patient.

Supplementary Figure 3. Quantitative RT-PCR plot in a control subject

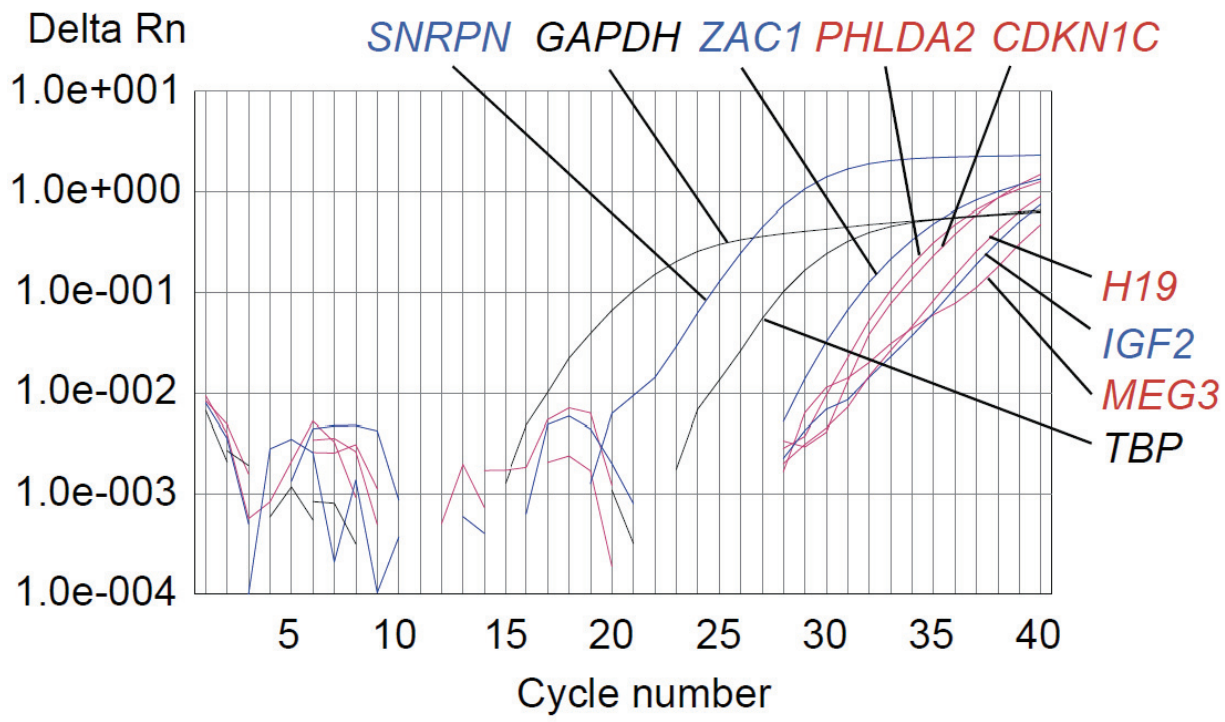

Paternally and maternally expressed genes are shown in blue and red, respectively.

SUPPLEMENTARY NOTE

Calculation of the ratio of cells with maternal uniparental isodisomy for all chromosomes (upid(AC)mat) in leukocytes and buccal epithelial cells

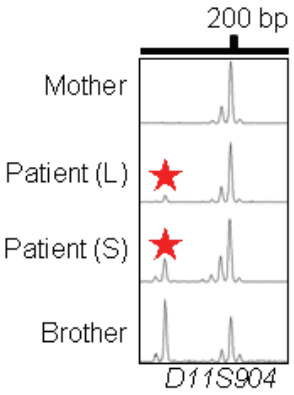

In this figure, two peaks are identified in the brother, and the area under curve (AUC) is larger for the short 184 bp peak than for the long 198 bp peak. This unequal amplification is consistent with short products being more easily amplified than long products. In the patient, the AUC ratio between the minor 184 bp peak of non-maternal origin and the major 198 bp peak of maternal origin is obtained as 0.09:1.0 for leukocytes (L) and 0.27:1.0 for salivary cells (S), after compensation of the unequal amplification between the two peaks, using the data in the brother.

Here, let "X" represent the frequency of the 46,XX upid(AC)mat cells in leukocytes (thus, (1 – X) denotes the frequency of 45,X cells in leukocytes). Then, the non-maternally (paternally) derived 184 bp peak is generated by one paternally derived chromosome in the 45,X cells, i.e., (1 – X), and the maternally derived 198 bp peak is formed by the products from two maternally derived homologous chromosomes in the 46,XX upid(AC)mat cells and one maternally derived chromosome in the 45,X cells, i.e., (2X + (1 – X)) = (X + 1). Thus, the AUC ratio between the two peaks is represented as (1 – X):(X + 1) = 0.09:1.0, and "X" is obtained as 0.835 (83.5%). Similarly, when "Y" represents the frequency of the 46,XX upid(AC)mat cells in salivary cells, "Y" is obtained as 0.574 (57.4%). Furthermore, when "Z" represents the frequency of the 46,XX upid(AC)mat cells in buccal epithelium cells, "Z" is obtained as 0.183 (18.3%) on the basis of the assumption that salivary cells comprises 40% of buccal epithelium cells and 60% of leukocytes.

We performed such calculations for all the informative loci, and the mean frequency is determined as 84% in leukocytes, 56% in saliva cells, and 18% in epithelial buccal cells, as described in the main text.

SUPPLEMENTARY REFERENCES

1. Ikari K, Onda H, Furushima K, Maeda S, Harata S, Takeda J. Establishment of an optimized set of 406 microsatellite markers covering the whole genome for the Japanese population. *J Hum Genet* 2001;**46**:207–10.
2. Yamazawa K, Kagami M, Nagai T, Kondoh T, Onigata K, Maeyama K, Hasegawa T, Hasegawa Y, Yamazaki T, Mizuno S, Miyoshi Y, Miyagawa S, Horikawa R, Matsuoka K, Ogata T. Molecular and clinical findings and their correlations in Silver-Russell syndrome: implications for a positive role of IGF2 in growth determination and differential imprinting regulation of the IGF2-H19 domain in bodies and placentas. *J Mol Med* 2008;**86**:1171–81.
3. Yamazawa K, Kagami M, Ogawa M, Horikawa R, Ogata T. Placental hypoplasia in maternal uniparental disomy for chromosome 7. *Am J Med Genet Part A* 2008;**146A**:514–6.
4. Kamikihara T, Arima T, Kato K, Matsuda T, Kato H, Douchi T, Nagata Y, Nakao M, Wake N. Epigenetic silencing of the imprinted gene ZAC by DNA methylation is an early event in the progression of human ovarian cancer. *Int J Cancer* 2005;**115**:690–700.
5. Sasaki K, Soejima H, Higashimoto K, Yatsuki H, Ohashi H, Yakabe S, Joh K, Niikawa N, Mukai T. Japanese and North American/European patients with Beckwith-Wiedemann syndrome have different frequencies of some epigenetic and genetic alterations. *Eur J Hum Genet* 2007;**15**:1205–10.
6. Kobayashi H, Sato A, Otsu E, Hiura H, Tomatsu C, Utsunomiya T, Sasaki H, Yaegashi N, Arima T. Aberrant DNA methylation of imprinted loci in sperm from oligospermic patients. *Hum Mol Genet* 2007;**16**:2542–51.
7. El-Maarri O, Seoud M, Coullin P, Herbiniaux U, Oldenburg J, Rouleau G, Slim R. Maternal alleles acquiring paternal methylation patterns in biparental complete hydatidiform moles. *Hum Mol Genet* 2003;**12**:1405–13.